Research Article

MOLECULAR PAIN

Molecular Pain
Volume 12: 1–12
© The Author(s) 2016
Reprints and permissions:
sagepub.co.uk/journalsPermissions.nav
DOI: 10.1177/1744806916633704
mpx.sagepub.com

SAGE

Connexin 43 contributes to ectopic orofacial pain following inferior alveolar nerve injury

Kaori Kaji, DDS[1], Masamichi Shinoda, DDS, PhD[2], Kuniya Honda, DDS, PhD[2], Syumpei Unno, PhD[2], Noriyoshi Shimizu, DDS, PhD[1] and Koichi Iwata, DDS, PhD[2]

Abstract

Background: Clinically, it is well known that injury of mandibular nerve fiber induces persistent ectopic pain which can spread to a wide area of the orofacial region innervated by the uninjured trigeminal nerve branches. However, the exact mechanism of such persistent ectopic orofacial pain is not still known. The present study was undertaken to determine the role of connexin 43 in the trigeminal ganglion on mechanical hypersensitivity in rat whisker pad skin induced by inferior alveolar nerve injury. Here, we examined changes in orofacial mechanical sensitivity following inferior alveolar nerve injury. Furthermore, changes in connexin 43 expression in the trigeminal ganglion and its localization in the trigeminal ganglion were also examined. In addition, we investigated the functional significance of connexin 43 in relation to mechanical allodynia by using a selective gap junction blocker (Gap27).

Results: Long-lasting mechanical allodynia in the whisker pad skin and the upper eyelid skin, and activation of satellite glial cells in the trigeminal ganglion, were induced after inferior alveolar nerve injury. Connexin 43 was expressed in the activated satellite glial cells encircling trigeminal ganglion neurons innervating the whisker pad skin, and the connexin 43 protein expression was significantly increased after inferior alveolar nerve injury. Administration of Gap27 in the trigeminal ganglion significantly reduced satellite glial cell activation and mechanical hypersensitivity in the whisker pad skin. Moreover, the marked activation of satellite glial cells encircling trigeminal ganglion neurons innervating the whisker pad skin following inferior alveolar nerve injury implies that the satellite glial cell activation exerts a major influence on the excitability of nociceptive trigeminal ganglion neurons.

Conclusions: These findings indicate that the propagation of satellite glial cell activation throughout the trigeminal ganglion via gap junctions, which are composed of connexin 43, plays a pivotal role in ectopic mechanical hypersensitivity in whisker pad skin following inferior alveolar nerve injury.

Keywords

Trigeminal ganglion, ectopic mechanical allodynia, satellite glial cell, inferior alveolar nerve injury, connexin 43, gap junction

Date received: 26 December 2015; accepted: 29 December 2015

Background

It is clinically known that injury of mandibular nerve by the extraction of a mandibular third molar or during maxillofacial surgery causes chronic orofacial pain that can spread to adjacent orofacial regions innervated by the uninjured trigeminal nerve branches.[1,2] In an effort to develop effective treatments for ectopic orofacial pain, we have developed a rodent model of mandibular nerve injury by performing inferior alveolar nerve (IAN) transection (IANX), which induces pain hypersensitivity in the whisker pad skin innervated by the uninjured trigeminal nerve branch.[3,4]

Peripherally, nitric oxide released from trigeminal ganglion (TG) neurons innervating the mandibular division (V3) following IANX was shown to enhance the excitability of TG neurons innervating the whisker pad skin, suggesting that the resulting TG neuronal hyperexcitability may underlie ectopic mechanical hypersensitivity in the whisker pad skin.[7] IANX was also found to cause an increase in transient receptor

[1]Department of Orthodontics, Nihon University School of Dentistry, Chiyoda-ku, Tokyo, Japan
[2]Department of Physiology, Nihon University School of Dentistry, Chiyoda-ku, Tokyo, Japan

Corresponding author:
Masamichi Shinoda, Department of Physiology, Nihon University School of Dentistry, 1-8-13 Kandasurugadai, Chiyoda-ku, Tokyo 101-8310, Japan.
Email: shinoda.masamichi@nihon-u.ac.jp

Creative Commons Non Commercial CC-BY-NC: This article is distributed under the terms of the Creative Commons Attribution-NonCommercial 3.0 License (http://www.creativecommons.org/licenses/by-nc/3.0/) which permits non-commercial use, reproduction and distribution of the work without further permission provided the original work is attributed as specified on the SAGE and Open Access pages (https://us.sagepub.com/en-us/nam/open-access-at-sage).

potential vanilloid 1 (TRPV1) which is a well-known contributor to heat nociceptive processing in TG neurons innervating the whisker pad skin, resulting the spreading of behavioral hypersensitivity following capsaicin injection to the adjacent whisker pad skin.[8] These studies indicate that intra-TG signaling plays an important role in the modulation of trigeminal nociceptive processes.

In the TG or dorsal root ganglion (DRG), satellite glial cells (SGCs) wrap completely around the soma of primary sensory neurons and can be identified by their morphological structure and the presence of glial fibrillary acidic protein (GFAP), which is nonexistent in neurons.[9,10] While barely detectable in SGCs under normal physiological conditions, GFAP immunoreactivity is dramatically enhanced in the SGCs by pathological states such as peripheral nerve injury, inflammation, or cancer, in parallel with some functional changes.[11–13] Therefore, enhanced GFAP immunoreactivity is commonly used as a marker of SGC reactivation.[9]

Gap junction is organized into two hemichannels, which are called connexons, and contribute to binding between cells.[14] Through gap junctions, the direct exchange of ions and small molecules proceeds between neighboring cells.[15] Connexin 43 (Cx43) is the primary gap junction protein, known to modulate the transport of small molecules between cells.[16] Along with an increase in the number of SGCs, the couplings between SGCs involved in the increase in the number of gap junctions are also increased following peripheral nerve injury.[17,18] Moreover, Cx43 in the TG increased following a chronic constriction injury of the infraorbital nerve, while depressing Cx43 expression using RNA interference recovered mechanical hypersensitivity in whisker pad skin.[19] These results imply that activation of SGCs in the TG influences the level of primary afferent neuronal excitability, which plays an important role in neuropathic pain conditions.

In this study, we examined changes in the mechanical sensitivity of the upper eyelid skin and whisker pad skin following IANX. Furthermore, changes in Cx43 expression in the TG and its localization in the TG were also examined. In addition, we investigated the functional significance of Cx43 in relation to mechanical allodynia by the intra-TG administration of a selective gap junction blocker, Gap27.

Methods

Animals

Male Sprague-Dawley rats ($n = 156$; Japan SLC, Shizuoka, Japan) weighing 160–270 g were used in this study. All rats were housed in clear polycarbonate cages (length × width × height = 48 × 26.5 × 21 cm) containing paper shavings as bedding and kept in a temperature-controlled room ($23 \pm 2^{\circ}$C) on a 12 h light/dark cycle (light on at 7:00, off at 19:00) with *ad libitum* access to food and water. All experiments were performed in accordance with the National Institutes of Health Guide for the Care and Use of Laboratory Animals and the guidelines of the International Association for the Study of Pain[54] and approved by the local animal ethics committee at Nihon University (AP15D011). The minimum number of animals was used in this study for statistical analysis.

Inferior alveolar nerve transection

To perform IANX, rats were deeply anesthetized with intraperitoneal (i.p.) sodium pentobarbital (50 mg/kg; Schering Plough, Whitehouse Station, NJ) and placed on a warm mat (37°C).[8,55] Briefly, the left facial skin over the masseter muscle was incised using a scalpel, and the masseter muscle was dissected to expose the alveolar bone. The surface of the alveolar bone covering the left IAN was removed to expose the IAN. The exposed IAN was lifted, transected, and repositioned in the mandibular canal without any discernable gap between the cut nerve ends. As a control, a sham operation was performed which was identical to that described above but without IANX. The incisions were closed using 6-0 silk sutures.

Mechanical sensitivity of the orofacial skin

Prior to behavioral testing, rats were trained daily for approximately one week to calmly protrude their snout from a cage that had a small opening in the front wall allowing the rats to freely remove their snout upon applied stimulation.[7,56] Once the rats were successfully trained, we applied mechanical stimuli to the upper eyelid skin (Territory of 1st branch of trigeminal nerve) or the whisker pad skin (Territory of 2nd branch of trigeminal nerve) using von Frey filaments (Touch Test Sensory Evaluator, North Coast Medical, Morgan Hill, CA) to measure mechanical head-withdrawal threshold (MHWT) bilateral to IANX and ipsilateral to sham-operated rats. The MHWT was chosen as the lowest pressure intensity that evoked withdrawal responses to three or more of five stimuli (duration: 1 s). Mechanical stimuli using von Frey filaments were applied to the upper eyelid skin or the whisker pad skin after IANX or sham operation for 14 days. All behavioral testing was performed under blinded conditions. The behavioral experiments were conducted in rats without any motor deficit.

Changes in mechanical hypersensitivity following Gap27 administration in the TG

Rats were anesthetized with sodium pentobarbital (50 mg/kg, i.p.) and placed in a stereotaxic apparatus. The skull was exposed and a small hole (diameter: 1 mm) was drilled directly above the location of the bifurcation between the 1st/2nd branches of the trigeminal nerve (V1/V2) region and the 3rd branch of the trigeminal nerve (V3) region of the TG. The guide cannula was extended in the TG ipsilateral to IANX or sham operation through the hole (9 mm below the skull surface, 2.8 mm anterior from the posterior fontanelle, 2.7 mm lateral to the sagittal suture) and was fixed to the skull with three stainless-steel screws and dental cement. After completion of the cannulation, the rats were allowed to recover for at least seven days before experiments were performed.

Gap27 (3 mM; Tocris Bioscience, Bristol, UK) were dissolved in physiological saline (vehicle). For continuous Gap27 or vehicle administration in the TG, rats were anesthetized with sodium pentobarbital (50 mg/kg, i.p.), and a 30-gauge injection needle was inserted in the TG 9.5 mm below the skull surface through the guide cannula. The injection needle was connected to an osmotic pump (ALZET Pump Model 2002, Durect, Cupertino, CA, USA; total volume, 200 µl) filled with Gap27 or vehicle by a soft microsilicon tube (0.8 mm in diameter), and the osmotic pump was embedded subcutaneously in the dorsal portion of the body. In this manner, Gap27 was continuously administered for nine days (0.5 µl/h, from day 0 to day 8) using the osmotic pump.

For single Gap27 or vehicle administration in the TG, a 30-gauge injection needle connected to a 10 µl Hamilton syringe was inserted in the TG 9.5 mm below the skull surface through the guide cannula under light anesthesia with 2% isoflurane in oxygen; 1 µl of Gap27 or vehicle was administered in the TG on day 4 after IANX or sham operation.

The MHWT was measured on days 1, 2, 4, 6, and 8 after IANX with continuous Gap27 administration in the TG or single Gap27 or vehicle administration in the TG as described earlier. The Cx43 and GFAP expression in V1-V2 and V3 of TG was also measured on day 8 after IANX with continuous Gap27 or vehicle administration in the TG as described above.

Immunohistochemistry

In advance, retrograde labeling tracer FluoroGold (FG; 4% hydroxystilbamidine) (Fluorochrome, Denver, CO) was dissolved in saline. Under deep anesthesia with sodium pentobarbital (50 mg/kg, i.p.), FG (10 µl) was injected into the skin of the left whisker pad with a 30-gauge needle during the IANX or sham operation. On day 8 after IANX or sham operation with continuous administration of Gap27 (3 mM) or vehicle in the TG, rats were anesthetized with sodium pentobarbital (50 mg/kg, i.p.) and transcardially perfused with saline followed by a fixative containing 4% paraformaldehyde in 0.1 M phosphate buffer (PB; pH 7.4). TGs were excised after perfusion and immersed in the same fixative for more than 4 h at 4°C, then transferred to 0.01 M phosphate buffered saline (PBS) containing 20% sucrose for 12 h for cryoprotection. TGs were embedded in Tissue Tek (Sakura Finetechnical, Tokyo, Japan) and stored at −20°C until cryosectioning. TGs were sectioned in the horizontal plane along the long axis at a thickness of 12 µm. Every 10th section was thaw-mounted on MAS-GP micro slide glass (Matsunami, Osaka, Japan) and dried overnight at room temperature. After rinsing with 0.01 M PBS, the sections were incubated with rabbit anti-Cx43 polyclonal antibody (1:200; Sigma–Aldrich, St. Louis, MO, USA) and mouse anti-GFAP monoclonal antibody (1:1000; Merck Millipore, Billerica, MA, USA) in 0.01 M PBS containing 4% normal goat serum and 0.3% Triton X-100 (Sigma–Aldrich) overnight at 4°C. After rinsing with 0.01 M PBS, sections were incubated in Alexa Fluor 568 anti-rabbit IgG (1:200; Thermo Fisher Scientific, Waltham, MA) and Alexa Fluor 488 anti-mouse IgG (1:200; Thermo Fisher Scientific) in 0.01 M PBS for 2 h at room temperature. After rinsing with 0.01 M PBS, sections were coverslipped in mounting medium (Thermo Fisher Scientific) and examined under a fluorescence microscope and analyzed using a BZ-9000 system (Keyence, Osaka, Japan). The number and the cell size of FG-labeled TG neurons encircled with GFAP-immunoreactive (IR) cells or GFAP-IR/Cx43-IR cells over 1/2 of the soma perimeters of TG neurons were measured (SensivMeasure; Mitani, Fukui, Japan). The percentage of FG-labeled TG neurons encircled with GFAP-IR cells and the percentage of FG-labeled TG neurons encircled with GFAP-IR or GFAP-IR/Cx43-IR cells in V2 and V3 were calculated by the following formula: 100×number of FG-labeled TG neurons encircled with GFAP-IR or GFAP-IR/Cx43-IR cells/total number of FG-labeled TG neurons. The calculation was performed on each group of cells classified by cell area. No specific labeling was observed in the absence of primary antibody under exactly the same conditions.

Western blotting

Under deep anesthesia with sodium pentobarbital (50 mg/kg, i.p.), the TG was excised and homogenized in ice-cold lysis buffer (137 mM NaCl; 20 mM Tris-HCl, pH 8.0; 1% NP40; 10% glycerol; 1 mM

phenylmethylsulfonyl fluoride; 10 μg/ml aprotinin; 1 g/ml leupeptin; 0.5 mM sodium vanadate) using a tube pestle (ThermoFisher Scientific) on days 1, 8 and 14 after IANX or sham operation and in naive rats. Similarly, the TGs of ophthalmic-maxillary division (V1-V2) and V3 were excised and homogenized on day 8 after IANX with continuous administration of Gap27 (3 mM) or vehicle in the TG. Following centrifugation at 15,000 rpm for 10 min at 4°C, the supernatants were transferred into new tubes, and the protein concentration was determined with a protein assay kit (Bio-Rad, Hercules, CA, USA). The supernatants were heat denatured in Laemmli sample buffer solution (Bio-Rad), and samples (containing 30 μg of protein) were subjected to electrophoresis on 10% SDS-PAGE and electroblotted onto polyvinylidene difluoride membranes (Trans-Blot Turbo Transfer Pack; Bio-Rad) using Trans-Blot Turbo (Bio-Rad). Following rinsing with Tris-buffered saline containing 0.1% Tween 20 (TBST), the membrane was incubated with 3% bovine serum albumin (BSA; Bovogen, Essendon, Australia). The membrane was incubated overnight at 4°C with rabbit anti-Cx43 polyclonal antibody (1:2000; Sigma–Aldrich) or mouse anti-GFAP monoclonal antibody (1:1000; Merck Millipore) diluted in TBST containing 3% BSA. Bound antibody was visualized using a horseradish peroxidase-conjugated donkey anti-rabbit antibody (cell signaling) or a horseradish peroxidase-conjugated rabbit anti-mouse antibody (Jackson ImmunoResearch, West Grove, PA, USA) and Western Lightning ELC Pro (PerikinElmer, Waltham, MA, USA). Band intensity was quantified using a ChemiDoc MP system (Bio-Rad) and normalized to β-actin on blots reprobed with anti-β-actin antibody (1:200; Santa Cruz, Santa Cruz, CA, USA) after removing bound protein using a stripping reagent (Thermo Scientific).

Statistical analysis

Data were expressed as mean ± SEM. Statistical analyses were performed by one-way analysis of variance (ANOVA) followed by Newman-Keuls's or Tukey's multiple-comparison tests. Two-way ANOVA with repeated-measures followed by Bonferroni's multiple-comparison tests was also used where appropriate. A value of $p < 0.05$ was defined as significant.

Results

Changes in mechanical sensitivity following IANX

The MHWT of the upper eyelid skin and the whisker pad skin ipsilateral to IANX was significantly decreased on day 1 after IANX compared to that of the skin contralateral to IANX or sham-operated rats, and the decreased MHWT persisted through to day 14 (Figure 1(a) and (b)). Moreover, the MHWT contralateral to IANX showed a delayed decrease on day 12 in the upper eyelid skin and on day 14 in the whisker pad skin after IANX comparing to that of sham-operated rats. Despite the presence of decreased MHWT in the upper eyelid skin and the whisker pad skin ipsilateral to IANX, rats gained weight normally during the experimental period.

Cx43 and GFAP expression in TG following IANX

On day 8 after IANX, Cx43 and GFAP were expressed in SGCs in the TG ipsilateral to IANX (Figure 2(a) to (c)). Cx43 protein expression in the TG ipsilateral to IANX significantly increased on day 8 after IANX relative to sham-operated or naive rats (naive, 4.8 ± 0.9; sham, 5.5 ± 0.9; IANX, 12.4 ± 2.2) (Figure 2(d)). GFAP protein expression in the TG ipsilateral to IANX significantly increased on day 8 after IANX relative to sham-operated rats and on days 1, 8, and 14 after IANX relative to naive rats (naive, 10.8 ± 1.7; IANX on day 1, 26.2 ± 4.1; IAN on day 8, 28.2 ± 1.2; IANX on day 14, 25.0 ± 3.1) (Figure 2(e)).

On day 8 after IANX or sham operation, FG-labeled TG neurons encircled with GFAP-IR and Cx43-IR cells were observed in TG of the maxillary division (V2) and the V3 (Figure 3(a)). On day 8 after IANX, the number of FG-labeled TG neurons encircled with GFAP-IR cells in V2 and V3 was significantly increased relative to sham-operated rats (GFAP-IR, V2: 41.2 ± 3.7%, V3: 47.5 ± 2.2%; GFAP-IR and Cx43-IR, V2: 31.4 ± 1.7%, V3: 37.3 ± 2.7%) (Figure 3(b)).

Effect of Gap27 administration in TG on mechanical allodynia following IANX

The effects of continuous Gap27 administration in the TG on mechanical allodynia in the upper eyelid skin and the whisker pad skin ipsilateral to IANX were tested on days 1, 2, 4, 6, and 8 after IANX. The continuous Gap27 administration in the TG produced a marked reversal of the mechanical allodynia after IANX from day 1 to day 8 when compared with that of sham-operated rats or IANX rats with vehicle administration in the TG (Figure 4(a) and (b)). The effects of a single Gap27 administration in the TG on day 4 after IANX on mechanical allodynia in the upper eyelid skin and the whisker pad skin ipsilateral to IANX were also tested on days 1, 2, 4, 5, 6, and 8 after IANX. The single Gap27 administration in the TG on day 4 after IANX produced a marked reversal of the mechanical allodynia on days 4 and 5 after IANX when compared with that of IAN-transected rats with vehicle administration in the TG (Figure 5(a) and (b)). Motor deficits or sedation were

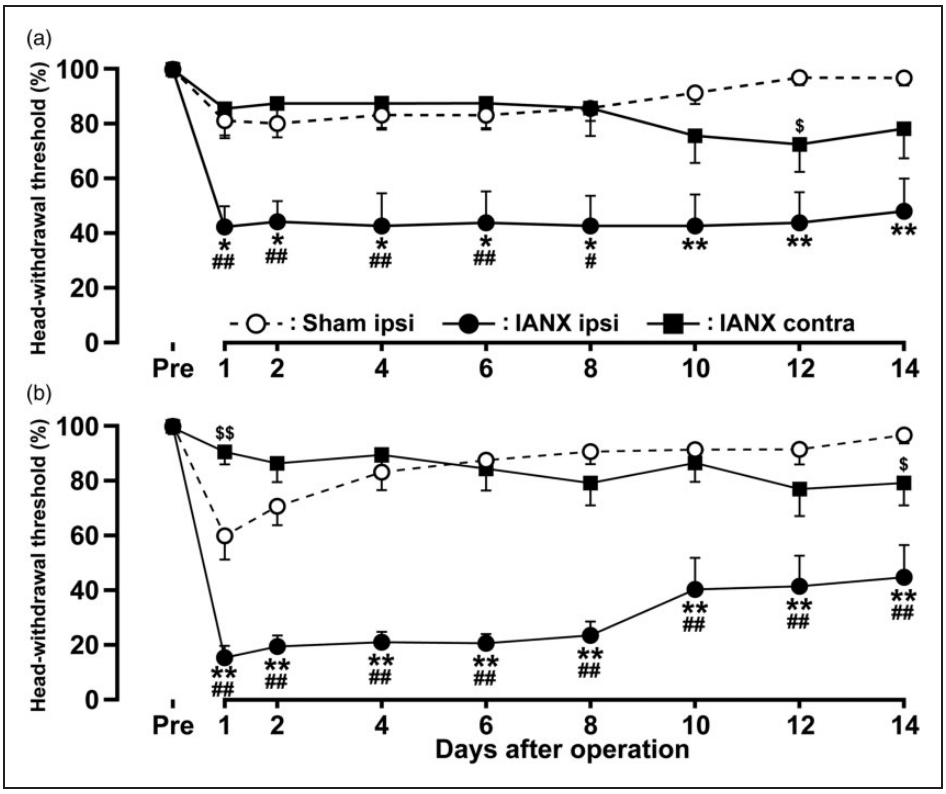

Figure 1. Changes in mechanical sensitivity following IANX. Bilateral MHWTs were measured in upper eyelid skin (a) and whisker pad skin (b) following IANX or sham operation. Data are expressed as percentage (mean ± SEM) of MHWT for each group, normalized to preoperation MHWT (100%). $^{\$}p < 0.05$, $^{\$\$}p < 0.01$, $^{*}p < 0.05$, $^{**}p < 0.01$; compared to sham-operated rats. $^{\#}p < 0.05$, $^{\#\#}p < 0.01$; compared to contralateral side. ($n = 8$ in each group; two-way ANOVA with repeated measures, followed by Bonferroni's multiple-comparison tests.)

not observed during the experimental period (data not shown).

Changes in Cx43 and GFAP expression in TG following Gap27 administration

FG-labeled TG neurons encircled with GFAP-IR and Cx43-IR cells were observed in naive rats (Figure 6(a)). On day 8 after IANX or sham operation, FG-labeled TG neurons encircled with GFAP-IR cells were observed in both sham-operated rats and IANX rats with or without intra-TG Gap27 administration (Figure 6(b) and (c)). The number of FG-labeled TG neurons encircled with GFAP-IR cells in the Gap27-administered group was significantly smaller than that of the vehicle-administered group on day 8 after IANX (naive: 21.2 ± 2.6%, IANX/vehicle: 48.6 ± 2.6%, IANX/Gap27: 26.4 ± 5.1%) (Figure 6(d)). The cell area analysis revealed that the number of FG-labeled TG neurons encircled with GFAP-IR cells was markedly increased in cell groups $\leq 199\,\mu m^2$ in area on day 8 in the Gap27-administered group (vehicle: 9.8 ± 3.1%, Gap27: 3.1 ± 1.6%) (Figure 6(e)). There was no significant difference in the number of FG-labeled TG neurons between IANX rats and sham-operated rats (data not shown).

On day 8 after IANX with continuous administration of Gap27 or vehicle in the TG, the expressions of Cx43 and GFAP in the V1-V2 or the V3 of TG were assessed by Western blotting of protein extracts. Relative Cx43 expression in both V1-V2 and V3 of TG in Gap27-administrated group was significantly lower than that of the vehicle-administrated group (vehicle: 6.7 ± 0.2, Gap27: 4.4 ± 0.1 in V1-V2; vehicle: 2.8 ± 0.2, Gap27: 2.4 ± 0.1 in V3) (Figure 7(a) and (b)). Similarly, GFAP expression in Gap27-administrated group was significantly lower than that of the vehicle-administrated group (vehicle: 4.0 ± 0.3, Gap27: 2.4 ± 0.4 in V1-V2; vehicle: 1.1 ± 0.1, Gap27: 0.7 ± 0.1 in V3) (Figure 7(c) and (d)).

Discussion

In previous studies, we demonstrated that mechanical hypersensitivity in region innervated by the uninjured second branch of the trigeminal nerve ipsilateral to IANX was caused by IANX.[5,6] In this study, long-lasting mechanical allodynia was induced not only in the

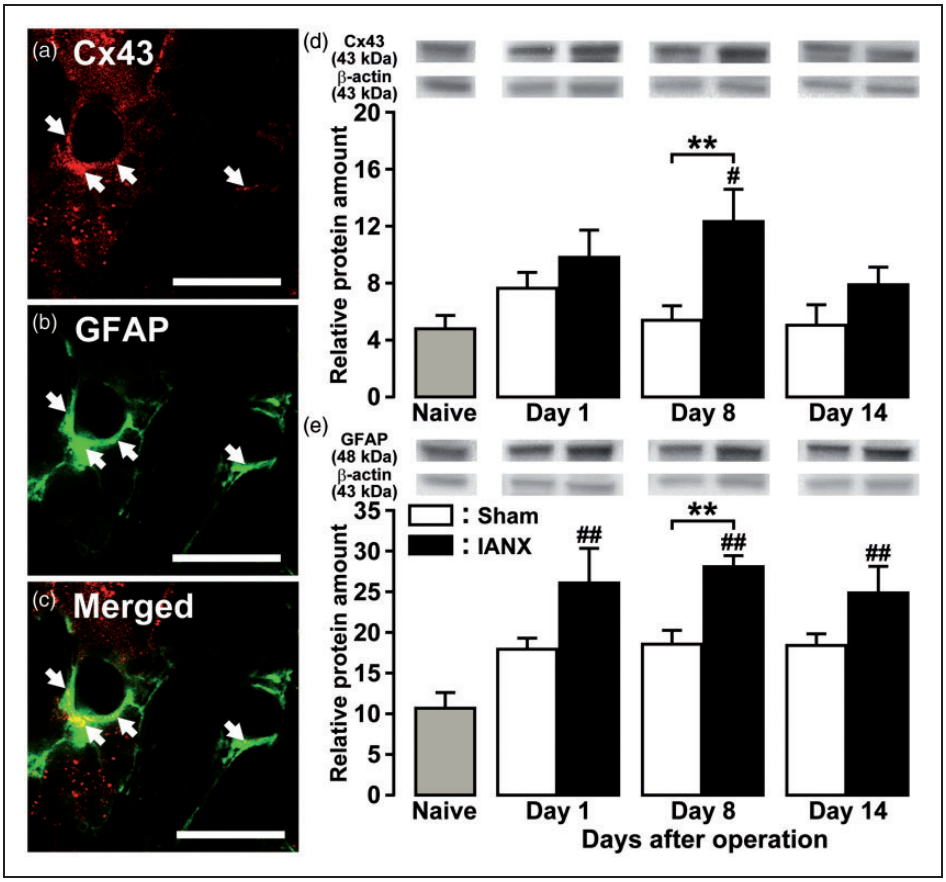

Figure 2. Cx43 and GFAP expression in TG following IANX. Photomicrographs of Cx43-IR cells (a), GFAP-IR cells (b), Cx43-IR and GFAP-IR cells (c) in TG on day 8 following IANX. Arrows denote double-IR cells. Scale bars: 50 μm. Relative amount of Cx43 (d) and GFAP protein (e) in the TG of naive rats and on days 1, 8, and 14 after IANX or sham operation. β-actin protein was used as loading control. Data represent mean ± SEM. $^{**}p < 0.01$: compared to sham-operated rats; $^{\#}p < 0.05$, $^{\#\#}p < 0.01$: compared to naive rats. ($n = 8$ in each group; one-way ANOVA followed by Newman-Keuls's multiple-comparison tests.)

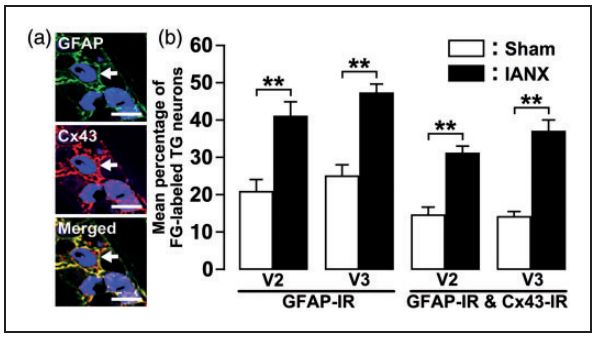

Figure 3. Cx43 and GFAP expression in TG of V2 and V3 following IANX. (a) Photomicrographs of Cx43-IR/GFAP-IR cells in TG of V3 on day 8 following IANX operation. Arrows denote double-IR cells. Scale bars: 50 μm. (b) Mean percentage of FG-labeled TG neurons encircled with GFAP-IR or Cx43-IR/GFAP-IR cells in TG of V2 and V3 on day 8 after IANX or sham operation. $^{**}p < 0.01$ ($n = 4$ in each group; one-way analysis of ANOVA followed by Tukey's multiple-comparison tests.)

whisker pad skin of rats but also in the ipsilateral upper eyelid skin after IANX. Enhanced 5-HT release from the rostral ventromedial medulla leads to enhanced activation of TRPV1 on the central terminals of primary afferents in the ipsilateral trigeminal subnucleus caudalis following infraorbital nerve injury, resulting in the ectopic orofacial pain associated with the central sensitization of injured and uninjured nerve fibers.[18]

Furthermore, a delayed induction in mechanical hypersensitivity was observed in the upper eyelid skin and the whisker pad skin contralateral to IANX when compared to that of sham-operated rats. Several studies in humans and experimental animal models of peripheral nerve injury indicate that some neural mechanisms at the spinal level are involved in bilateral pain hypersensitivity.[19–22] Recent studies suggest possible mechanisms of contralateral pain hypersensitivity following peripheral nerve injury. Newly sprouted neurites and ectopic synapses in the contralateral DRG are induced by nerve

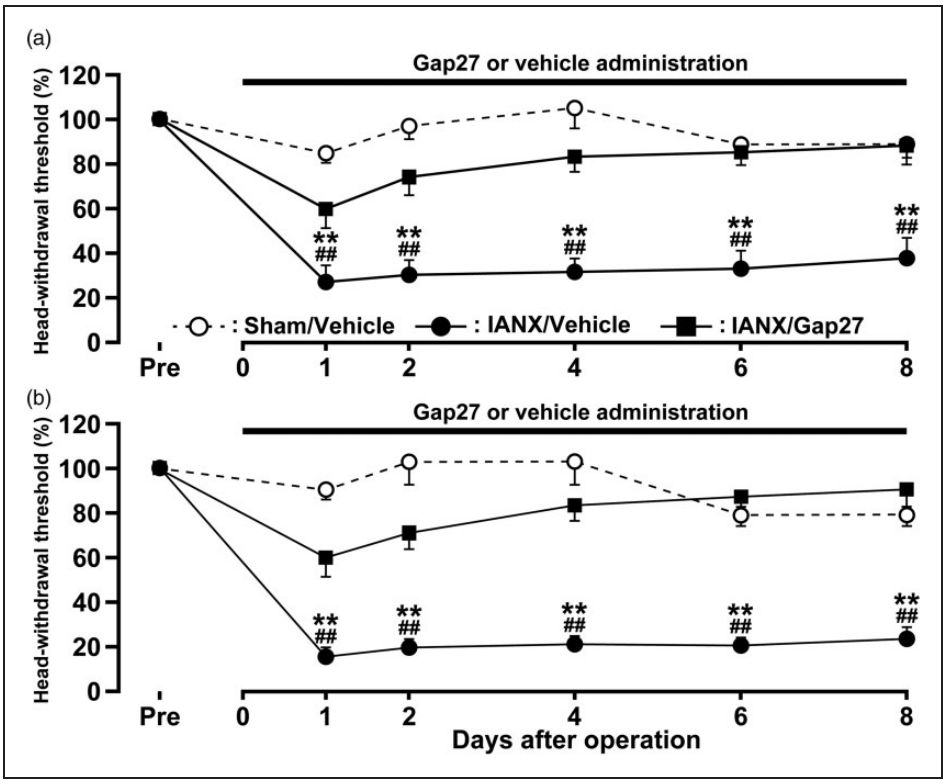

Figure 4. Effects of TG continuous-administration of Gap 27 on mechanical sensitivity in the orofacial region following IANX. Time course of changes in MHWT in upper eyelid skin (a) and whisker pad skin (b) in sham-operated or IANX rats with intra-TG Gap 27 or vehicle administration. Error bars indicate SEM. $^{\#\#}p < 0.01$ vs. prevalue; $^{**}p < 0.01$ vs. value of IANX group with TG continuous-administration of Gap 27. ($n = 8$ in each group; two-way ANOVA with repeated measures followed by Bonferroni's multiple-comparison tests.)

growth factor produced in the contralateral DRG after peripheral nerve injury, leading to the development of chronic mirror-image pain.[23] Moreover, microglia are activated in the Vc receiving noxious inputs from the orofacial region following peripheral trigeminal nerve injury.[24,25] Activated microglia release signaling molecules such as tumor necrosis factor-alpha, interleukin-1β, and brain-derived neurotrophic factor, which induce the hyperactivity of secondary neurons, resulting in the development of bilateral mechanical allodynia.[26] Although microglial activation is induced in the bilateral spinal trigeminal nucleus following trigeminal nerve injury, contralateral microglial activation is delayed and weak.[5,29] Together, these results suggest that bilateral mechanical hypersensitivity induced in the entire orofacial region by IANX involves microglial activation in the bilateral spinal trigeminal nucleus. And, a difference in the activation pattern of bilateral microglia may also explain the relative delay and the smaller magnitude of mechanical hypersensitivity contralateral to IANX. However, the mechanisms of transmedial activation in microglia attributable to peripheral trigeminal nerve injury are still unclear, and further studies are needed.

Changes in cell coupling resulting from pathological conditions are caused by alterations in connexin expression, and the subsequent modulations of intercellular communication depend on gap junctions.[30] Cx43, the major structural component of gap junctions, is expressed in glial cells, and its expression was shown to be upregulated following peripheral nerve injury[15,31] The phosphorylation of extracellular signal-regulated kinase (ERK) and p38 are induced in SGCs following chronic constriction injury of the sciatic nerve.[32] Additionally, Janus kinase 2 (JAK2) phosphorylation in SGCs in DRG was upregulated in animal models of ischemic injury.[33] Activation of the JAK/signal transducer and activator of transcription (JAK/STAT) pathway in astrocytes increases Cx43 expression and intercellular communication.[34] Cx43 expression and activity of intercellular communication depending on gap junction were also enhanced via protein kinase C (PKC)-ERK signaling cascade.[35] Here, Cx43 was expressed in the activated SGCs in ipsilateral TG, and the Cx43 protein expression

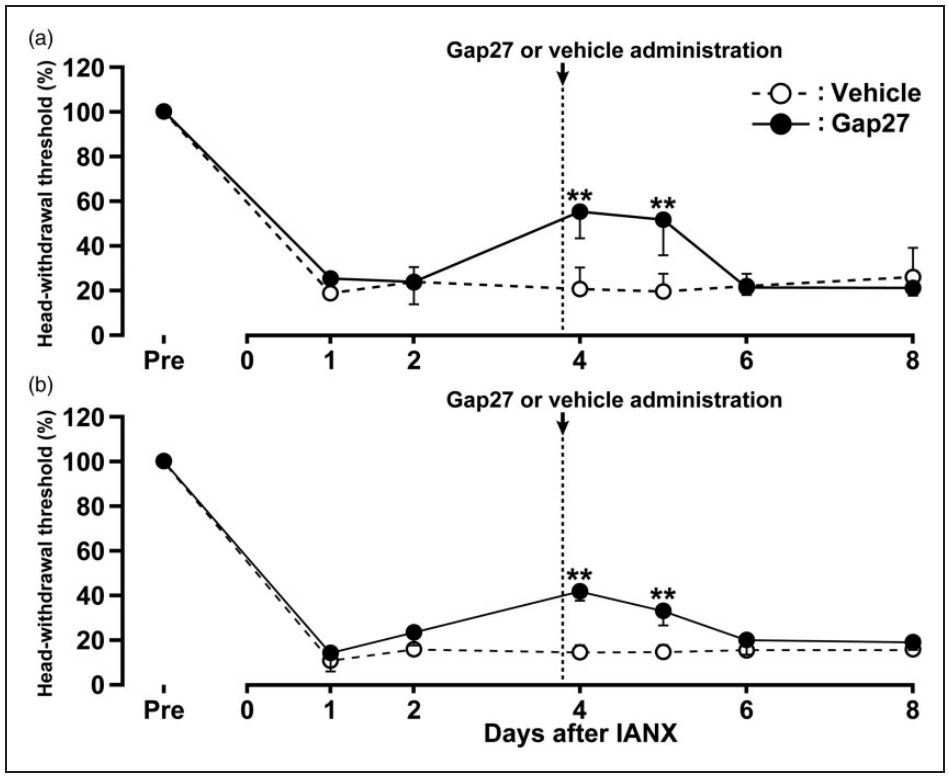

Figure 5. Effects of TG single-administration of Gap 27 on mechanical sensitivity in the orofacial region following IANX. Time course of changes in MHWT in upper eyelid skin (a) and whisker pad skin (b) in sham-operated or IANX rats with intra-TG Gap 27 or vehicle administration. Error bars indicate SEM. $^{**}p < 0.01$ ($n = 8$ in each group; two-way ANOVA with repeated measures followed by Bonferroni's multiple-comparison tests).

was significantly increased on day 8 after IANX. Taken together, we hypothesize that the enhancement of Cx43 expression in the activated SGCs following IANX may have been induced via JAK/STAT or PKC-ERK signaling cascades. However, further studies to identify the cells which express Cx43 and gap junctions may be needed because the immunohistochemical techniques we used cannot exactly establish the presence of Cx43 and gap junctions in SGCs.

In this study, GFAP expression in TG and the Cx43 expression in activated SGCs which encircle TG neurons in V2 and V3 were increased, suggesting that activation of Cx43-expressed SGCs spread throughout the TG following IANX. The activation of SGCs and the Cx43 expression in both V1-V2 and V3 in TG were significantly depressed by continuous Gap27 intra-TG administration. Moreover, continuous Gap27 intra-TG administration also depressed mechanical hypersensitivity in the whisker pad skin. Gap junctions join adjacent glial cells and permit the passage of small molecules between adjacent glial cells.[36–39] Of these, calcium ions (Ca^{2+}) are continuously able to pass between adjacent glial cells through gap junctions, which initiate intercellular calcium waves (ICWs) between glial cells.[40,41] In SGCs in the TG, ICWs induce intracellular Ca^{2+} elevation which elicits glutamate release, reduction of inwardly rectifying potassium channel 4.1 (Kir4.1) expression, and activates small-conductance calcium-activated potassium channel 3 (SK3).[37,42,43] Glutamate signaling in TG neurons via metabotropic glutamate receptor 5 (mGluR5) increases neuronal excitation and leads to mechanical allodynia in the orofacial region.[44] Moreover, a deficiency in potassium ion (K^+) buffering mediated by activated SGCs due to the reduction of Kir4.1, and the activation of SK3 will cause an increase in extracellular K^+, resulting in neuronal hyperexcitability.[17] Taken together with previous data, present findings suggest that the propagation of SGC activation throughout the TG via increased expression of gap junctions composed of Cx43 following IANX enhances TG neuronal excitability, resulting in ectopic mechanical hypersensitivity in the whisker pad skin.

Several studies indicate that the activated astrocytes and its gap junctions composed of Cx43 in central never system also contributes to the development of neuronal hyperexcitability that underlies persistent pain following trigeminal nerve injury or inflammation.[3,45–47] Cx43 is abundantly expressed in astrocytes and Cx43 expression is increased after peripheral nerve injury.[48,16]

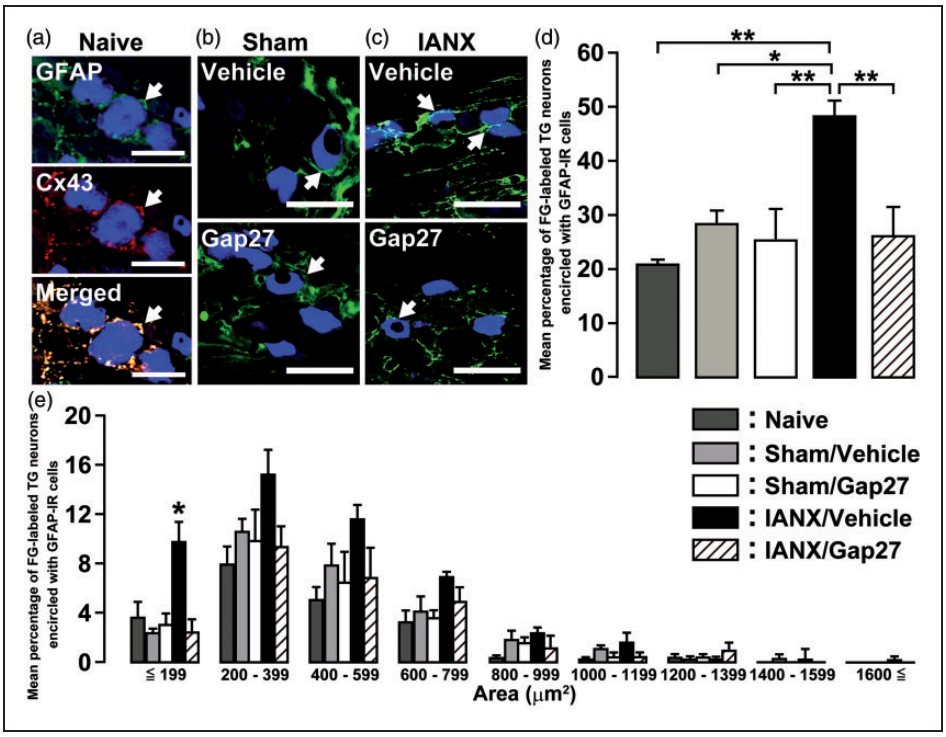

Figure 6. Effect of continuous-Gap 27 administration on SGC activation in TG after IANX. Photomicrographs of GFAP-IR and Cx43-IR cells encircled with FG-labeled TG neurons in naive rats (a), and GFAP-IR cells encircling FG-labeled TG neurons innervating the whisker pad skin on day 8 following sham operation (b) or IANX (c) with continuous administration of vehicle or Gap 27. Arrows denote FG-labeled TG neurons. Scale bars: 50 μm. Mean percentages (d) and size-frequency histograms illustrating distribution (e) of FG-labeled TG neurons encircled with GFAP-IR cells on day 8 after sham operation or IANX with continuous administration of vehicle or Gap 27. $^{*}p < 0.05$, $^{**}p < 0.01$ ($n = 4$ in each group; one-way analysis of ANOVA followed by Tukey's multiple-comparison tests).

Intrathecal (i.t.) administration of gap junction blocker attenuates the mechanical allodynia in whisker pad skin as well as the accompanying central sensitization of nociceptive neurons in medullary dorsal horn (MDH) induced by infraorbital nerve injury.[49] Enhanced MDH neuronal excitability by tooth pulp inflammation was completely suppressed by i.t. gap junction blocker administration.[50] These findings indicate that astroglial gap junctions composed of Cx43 in MDH play an important role in pain hypersensitivity in the orofacial region.

Small-sized primary afferent neurons include not only nociceptive afferents but also non-nociceptive thermosensitive afferents.[51] The number of activated SGCs which encircle the small TG neurons ($\leq 199\,\mu m^2$ in area) innervating the whisker pad skin was markedly increased following IANX, and therefore, it is possible that activation of SGCs exerts a major influence on the excitability of small TG neurons, though changes in non-nociceptive thermosensitivity can scarcely be denied. Generally, small-diameter neurons in the DRG or TG elongate slowly conducting unmyelinated (C) or thinly myelinated (Aδ) axons closely associated with nociception.[52] Interestingly, the mGluR5 receptor is predominantly expressed in small diameter rat DRG neurons,[53] providing further evidence that glutamate signaling in TG neurons via mGluR5 may play an important role in TG neuronal hyperexcitability and the subsequent mechanical allodynia in whisker pad skin. Additionally, the single Gap27 administration in the TG temporarily produced a marked reversal of the mechanical allodynia in the whisker pad skin on day 4 after IANX. This result implies that activated SGCs persistently elicit glutamate release or a deficiency in K^+ buffering, resulting in the persistent enhancement of TG neuronal excitability.

Conclusion

We have shown that the propagation of SGC activation throughout the TG following IANX via gap junctions which are composed of Cx43, resulting in ectopic mechanical hypersensitivity in both whisker pad skin and the eyelid skin. By the same token, administration of Gap27 in the TG significantly reduced SGC activation and the mechanical hypersensitivity. Thus, activation of SGCs throughout sensory ganglion via gap junctions may be a promising therapeutic target for treating ectopic pain associated with peripheral nerve injury.

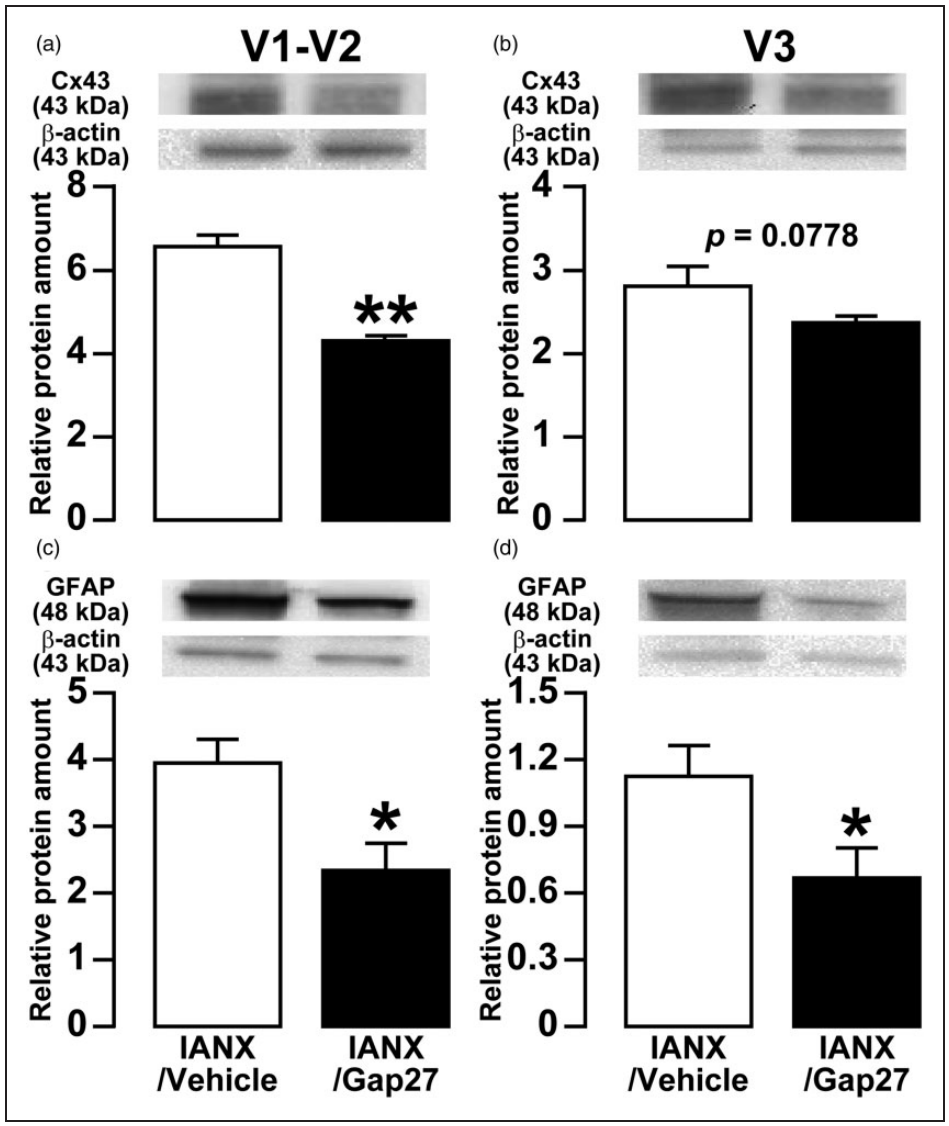

Figure 7. Effects of TG continuous-administration of Gap 27 on Cx43 and GFAP expression in TG following IANX. Relative amount of Cx43 protein in the V1-V2 (a) and V3 (b) of TG, and relative amount of GFAP protein in the V1-V2 (c) and V3 (d) of TG on day 8 after IANX. β-actin protein was used as loading control. Data represent mean ± SEM. *$p < 0.05$, **$p < 0.01$ ($n = 8$ in each group; Student's *t*-test).

Authors' contributions

KK, KH, SU, NS performed animal experiments, immunohistochemistry, western blotting and pharmacological testing and analyzed data; MS, KI designed experiments, supervised research and wrote the manuscript. All authors read and approved the final manuscript.

Declaration of Conflicting Interests

The author(s) declared no potential conflicts of interest with respect to the research, authorship, and/or publication of this article.

Funding

The author(s) disclosed receipt of the following financial support for the research, authorship, and/or publication of this article: This study was supported in part by research grants from Sato and Uemura Funds from the Nihon University School of Dentistry, a grant from the Dental Research Center in Nihon University School of Dentistry and from KAKENHI (Grant-in-Aid for Challenging Exploratory Research 15K15748, Grant-in-Aid for Scientific Research [C] 25860430 and 26463101) and MEXT-Supported Program for the Strategic Research Foundation at Private Universities 2013-2017.

References

1. Renton T, Yilmaz Z and Gaballah K. Evaluation of trigeminal nerve injuries in relation to third molar surgery in a prospective patient cohort. Recommendations for prevention. *Int J Oral Maxillofac Surg* 2012; 41: 1509–1518.
2. Khawaja N and Renton T. Case studies on implant removal influencing the resolution of inferior alveolar nerve injury. *Br Dent J* 2009; 206: 365–370.
3. Okada-Ogawa A, Suzuki I, Sessle BJ, et al. Astroglia in medullary dorsal horn (trigeminal spinal subnucleus caudalis) are involved in trigeminal neuropathic pain mechanisms. *J Neurosci* 2009; 29: 11161–11171.
4. Okada-Ogawa A, Nakaya Y, Imamura Y, et al. Involvement of medullary GABAergic system in extraterritorial neuropathic pain mechanisms associated with inferior alveolar nerve transection. *Exp Neurol* 2015; 267: 42–52.
5. Piao ZG, Cho IH, Park CK, et al. Activation of glia and microglial p38 MAPK in medullary dorsal horn contributes to tactile hypersensitivity following trigeminal sensory nerve injury. *Pain* 2006; 121: 219–231.
6. Zhang ZJ, Dong YL, Lu Y, et al. Chemokine CCL2 and its receptor CCR2 in the medullary dorsal horn are involved in trigeminal neuropathic pain. *J Neuroinflammation* 2012; 9: 136.
7. Sugiyama T, Shinoda M, Watase T, et al. Nitric oxide signaling contributes to ectopic orofacial neuropathic pain. *J Dent Res* 2013; 92: 1113–1117.
8. Hitomi S, Shinoda M, Suzuki I, et al. Involvement of transient receptor potential vanilloid 1 in ectopic pain following inferior alveolar nerve transection in rats. *Neurosci Lett* 2012; 513: 95–99.
9. Hanani M. Satellite glial cells in sensory ganglia: from form to function. *Brain Res Brain Res Rev* 2005; 48: 457–476.
10. Woodham P, Anderson PN, Nadim W, et al. Satellite cells surrounding axotomised rat dorsal root ganglion cells increase expression of a GFAP-like protein. *Neurosci Lett* 1989; 98: 8–12.
11. Hironaka K, Ozaki N, Hattori H, et al. Involvement of glial activation in trigeminal ganglion in a rat model of lower gingival cancer pain. *Nagoya J Med Sci* 2014; 76: 323–332.
12. Liu FY, Sun YN, Wang FT, et al. Activation of satellite glial cells in lumbar dorsal root ganglia contributes to neuropathic pain after spinal nerve ligation. *Brain Res* 2012; 1427: 65–77.
13. Matsuura S, Shimizu K, Shinoda M, et al. Mechanisms underlying ectopic persistent tooth-pulp pain following pulpal inflammation. *PLoS One* 2013; 8: e52840.
14. Hansson E and Skioldebrand E. Coupled cell networks are target cells of inflammation, which can spread between different body organs and develop into systemic chronic inflammation. *J Inflamm (Lond)* 2015; 12: 44.
15. Bennett MV, Garre JM, Orellana JA, et al. Connexin and pannexin hemichannels in inflammatory responses of glia and neurons. *Brain Res* 2012; 1487: 3–15.
16. Chen MJ, Kress B, Han X, et al. Astrocytic CX43 hemichannels and gap junctions play a crucial role in development of chronic neuropathic pain following spinal cord injury. *Glia* 2012; 60: 1660–1670.
17. Vit JP, Jasmin L, Bhargava A, et al. Satellite glial cells in the trigeminal ganglion as a determinant of orofacial neuropathic pain. *Neuron Glia Biol* 2006; 2: 247–257.
18. Pannese E, Ledda M, Cherkas PS, et al. Satellite cell reactions to axon injury of sensory ganglion neurons: increase in number of gap junctions and formation of bridges connecting previously separate perineuronal sheaths. *Anat Embryol (Berl)* 2003; 206: 337–347.
19. Ohara PT, Vit JP, Bhargava A, et al. Evidence for a role of connexin 43 in trigeminal pain using RNA interference in vivo. *J Neurophysiol* 2008; 100: 3064–3073.
20. Kim YS, Chu Y, Han L, et al. Central terminal sensitization of TRPV1 by descending serotonergic facilitation modulates chronic pain. *Neuron* 2014; 81: 873–887.
21. Arguis MJ, Perez J, Martinez G, et al. Contralateral neuropathic pain following a surgical model of unilateral nerve injury in rats. *Reg Anesth Pain Med* 2008; 33: 211–216.
22. Wasner G, Naleschinski D, Binder A, et al. The effect of menthol on cold allodynia in patients with neuropathic pain. *Pain Med* 2008; 9: 354–358.
23. Hatashita S, Sekiguchi M, Kobayashi H, et al. Contralateral neuropathic pain and neuropathology in dorsal root ganglion and spinal cord following hemilateral nerve injury in rats. *Spine (Phila Pa 1976)* 2008; 33: 1344–1351.
24. Nomura H, Ogawa A, Tashiro A, et al. Induction of Fos protein-like immunoreactivity in the trigeminal spinal nucleus caudalis and upper cervical cord following noxious and non-noxious mechanical stimulation of the whisker pad of the rat with an inferior alveolar nerve transection. *Pain* 2002; 95: 225–238.
25. Cheng CF, Cheng JK, Chen CY, et al. Nerve growth factor-induced synapse-like structures in contralateral sensory ganglia contribute to chronic mirror-image pain. *Pain* 2015; 156: 2295–2309.
26. Shibuta K, Suzuki I, Shinoda M, et al. Organization of hyperactive microglial cells in trigeminal spinal subnucleus caudalis and upper cervical spinal cord associated with orofacial neuropathic pain. *Brain Res* 2012; 1451: 74–86.
27. Terayama R, Fujisawa N, Yamaguchi D, et al. Differential activation of mitogen-activated protein kinases and glial cells in the trigeminal sensory nuclear complex following lingual nerve injury. *Neurosci Res* 2011; 69: 100–110.
28. Taves S, Berta T, Chen G, et al. Microglia and spinal cord synaptic plasticity in persistent pain. *Neural Plast* 2013; 2013: 753656.
29. Ma F, Zhang L, Oz HS, et al. Dysregulated TNFalpha promotes cytokine proteome profile increases and bilateral orofacial hypersensitivity. *Neuroscience* 2015; 300: 493–507.
30. Chew SS, Johnson CS, Green CR, et al. Role of connexin43 in central nervous system injury. *Exp Neurol* 2010; 225: 250–261.
31. Neumann E, Hermanns H, Barthel F, et al. Expression changes of microRNA-1 and its targets Connexin 43 and brain-derived neurotrophic factor in the peripheral nervous system of chronic neuropathic rats. *Mol Pain* 2015; 11: 39.

32. Obata K, Yamanaka H, Dai Y, et al. Differential activation of MAPK in injured and uninjured DRG neurons following chronic constriction injury of the sciatic nerve in rats. *Eur J Neurosci* 2004; 20: 2881–2895.
33. Campana WM and Myers RR. Exogenous erythropoietin protects against dorsal root ganglion apoptosis and pain following peripheral nerve injury. *Eur J Neurosci* 2003; 18: 1497–1506.
34. Ozog MA, Bernier SM, Bates DC, et al. The complex of ciliary neurotrophic factor-ciliary neurotrophic factor receptor alpha up-regulates connexin43 and intercellular coupling in astrocytes via the Janus tyrosine kinase/signal transducer and activator of transcription pathway. *Mol Biol Cell* 2004; 15: 4761–4774.
35. Lin PC, Shen CC, Liao CK, et al. HYS-32, a novel analogue of combretastatin A-4, enhances connexin43 expression and gap junction intercellular communication in rat astrocytes. *Neurochem Int* 2013; 62: 881–892.
36. Huang TY, Cherkas PS, Rosenthal DW, et al. Dye coupling among satellite glial cells in mammalian dorsal root ganglia. *Brain Res* 2005; 1036(1–2): 42–49.
37. Weick M, Cherkas PS, Hartig W, et al. P2 receptors in satellite glial cells in trigeminal ganglia of mice. *Neuroscience* 2003; 120: 969–977.
38. De Pina-Benabou MH, Srinivas M, Spray DC, et al. Calmodulin kinase pathway mediates the K+-induced increase in Gap junctional communication between mouse spinal cord astrocytes. *J Neurosci* 2001; 21: 6635–6643.
39. Scemes E, Suadicani SO and Spray DC. Intercellular communication in spinal cord astrocytes: fine tuning between gap junctions and P2 nucleotide receptors in calcium wave propagation. *J Neurosci* 2000; 20: 1435–1445.
40. Scemes E and Giaume C. Astrocyte calcium waves: what they are and what they do. *Glia* 2006; 54: 716–725.
41. Giugliano M. Calcium waves in astrocyte networks: theory and experiments. *Front Neurosci* 2009; 3: 160–161.
42. Wagner L, Warwick RA, Pannicke T, et al. Glutamate release from satellite glial cells of the murine trigeminal ganglion. *Neurosci Lett* 2014; 578: 143–147.
43. Vit JP, Ohara PT, Bhargava A, et al. Silencing the Kir4.1 potassium channel subunit in satellite glial cells of the rat trigeminal ganglion results in pain-like behavior in the absence of nerve injury. *J Neurosci* 2008; 28: 4161–4171.
44. Chung MK, Lee J, Joseph J, et al. Peripheral group I metabotropic glutamate receptor activation leads to muscle mechanical hyperalgesia through TRPV1 phosphorylation in the rat. *J Pain* 2015; 16: 67–76.
45. Ren K and Dubner R. Activity-triggered tetrapartite neuron-glial interactions following peripheral injury. *Curr Opin Pharmacol* 2015; 26: 16–25.
46. Lu Y, Jiang BC, Cao DL, et al. TRAF6 upregulation in spinal astrocytes maintains neuropathic pain by integrating TNF-alpha and IL-1beta signaling. *Pain* 2014; 155: 2618–2629.
47. Liu X, Tian Y, Lu N, et al. Stat3 inhibition attenuates mechanical allodynia through transcriptional regulation of chemokine expression in spinal astrocytes. *PLoS One* 2013; 8: e75804.
48. Nagy JI, Dudek FE and Rash JE. Update on connexins and gap junctions in neurons and glia in the mammalian nervous system. *Brain Res Brain Res Rev* 2004; 47: 191–215.
49. Wang H, Cao Y, Chiang CY, et al. The gap junction blocker carbenoxolone attenuates nociceptive behavior and medullary dorsal horn central sensitization induced by partial infraorbital nerve transection in rats. *Pain* 2014; 155: 429–435.
50. Chiang CY, Li Z, Dostrovsky JO, et al. Central sensitization in medullary dorsal horn involves gap junctions and hemichannels. *Neuroreport* 2010; 21: 233–237.
51. Numazaki M and Tominaga M. Nociception and TRP Channels. *Curr Drug Targets CNS Neurol Disord* 2004; 3: 479–485.
52. Gold MS and Gebhart GF. Nociceptor sensitization in pain pathogenesis. *Nat Med* 2010; 16: 1248–1257.
53. Valerio A, Rizzonelli P, Paterlini M, et al. mGluR5 metabotropic glutamate receptor distribution in rat and human spinal cord: a developmental study. *Neurosci Res* 1997; 28: 49–57.
54. Zimmermann M. Ethical guidelines for investigations of experimental pain in conscious animals. *Pain* 1983; 16: 109–110.
55. Saito K, Hitomi S, Suzuki I, et al. Modulation of trigeminal spinal subnucleus caudalis neuronal activity following regeneration of transected inferior alveolar nerve in rats. *J Neurophysiol* 2008; 99: 2251–2263.
56. Kitagawa J, Takeda M, Suzuki I, et al. Mechanisms involved in modulation of trigeminal primary afferent activity in rats with peripheral mononeuropathy. *Eur J Neurosci* 2006; 24: 1976–1986.